






ORIGINAL RESEARCH

Cardiovascular Development and Congenital Heart Disease Modeling in the Pig

George C. Gabriel, BS; William Devine, BS; Bethany K. Redel, PhD; Kristin M. Whitworth , PhD; Melissa Samuel, BS; Lee D. Spate, BS; Raissa F. Cecil, MS; Randall S. Prather , PhD; Yijen Wu , PhD; Kevin D. Wells , PhD; Cecilia W. Lo , PhD

BACKGROUND: Modeling cardiovascular diseases in mice has provided invaluable insights into the cause of congenital heart disease. However, the small size of the mouse heart has precluded translational studies. Given current high-efficiency gene editing, congenital heart disease modeling in other species is possible. The pig is advantageous given its cardiac anatomy, physiology, and size are similar to human infants. We profiled pig cardiovascular development and generated genetically edited pigs with congenital heart defects.

METHODS AND RESULTS: Pig conceptuses and fetuses were collected spanning 7 stages (day 20 to birth at day 115), with at least 3 embryos analyzed per stage. A combination of magnetic resonance imaging and 3-dimensional histological reconstructions with episcopic confocal microscopy were conducted. Gross dissections were performed in late-stage or term fetuses by using sequential segmental analysis of the atrial, ventricular, and arterial segments. At day 20, the heart has looped, forming a common atria and ventricle and an undivided outflow tract. Cardiac morphogenesis progressed rapidly, with atrial and outflow septation evident by day 26 and ventricular septation completed by day 30. The outflow and atrioventricular cushions seen at day 20 undergo remodeling to form mature valves, a process continuing beyond day 42. Genetically edited pigs generated with mutation in chromatin modifier *SAP130* exhibited tricuspid dysplasia, with tricuspid atresia associated with early embryonic lethality.

CONCLUSIONS: The major events in pig cardiac morphogenesis are largely complete by day 30. The developmental profile is similar to human and mouse, indicating gene edited pigs may provide new opportunities for preclinical studies focused on outcome improvements for congenital heart disease.

Key Words: congenital heart disease ■ CRISPR gene editing ■ heart development ■ pig model

Animal modeling has been invaluable for investigating the cause of human disease. Insights emerging from animal models can provide the basis for the development of new diagnostic tests or the design of evidence-based therapies to improve disease outcome. Although disease modeling using transgenic mice has been readily available, this process has been more problematic for larger animals, such as the pig, until recent advances in CRISPR gene

editing technologies. Gene editing has streamlined the production of animal models, with genetically engineered pigs now coming into more prominence.^{1,2} Pig models are particularly compelling for investigating cardiovascular diseases, as human and pig not only have a similar 4-chamber cardiovascular anatomy, but also exhibit similar cardiac physiology. This contrasts with rodent models with similar 4-chamber anatomy but markedly different cardiac physiology.^{3,4} Thus, mice

Correspondence to: Cecilia W. Lo, PhD, Department of Developmental Biology, University of Pittsburgh School of Medicine, 530 45th St, 8120 Rangos Research Center, Pittsburgh, PA 15201. E-mail: cel36@pitt.edu

Supplementary material for this article is available at <https://www.ahajournals.org/doi/suppl/10.1161/JAHA.121.021631>

For Sources of Funding and Disclosures, see page 15.

© 2021 The Authors. Published on behalf of the American Heart Association, Inc., by Wiley. This is an open access article under the terms of the Creative Commons Attribution-NonCommercial-NoDerivs License, which permits use and distribution in any medium, provided the original work is properly cited, the use is non-commercial and no modifications or adaptations are made.

JAHA is available at: www.ahajournals.org/journal/jaha

CLINICAL PERSPECTIVE

What Is New?

- This study presents the first comprehensive cardiovascular development atlas in the pig, spanning gestation day 20 to term.
- This study provides a comparative guide to the staging of pig, mouse, and human heart development.
- This study describes production of the first CRISPR gene edited pigs with congenital heart disease characterized by tricuspid dysplasia.

What Are the Clinical Implications?

- Availability of pig models of congenital heart disease would allow the pursuit of surgical and clinical outcome studies not feasible with rodent models.
- Pig models of congenital heart disease would provide the means to develop and test ventricular assist devices optimized for infants as a bridge to heart transplantation.
- Pig models of congenital heart disease can provide invaluable opportunities to train surgeons on congenital cardiac surgical procedures.

Nonstandard Abbreviations and Acronyms

HLHS hypoplastic left heart syndrome

have little kinetic reserve, exhibiting a resting heart rate 10× higher than humans. Mice are only able to elevate heart rate up to 50% maximally compared with up to 300% in humans.⁵ As kinetic reserve is often impacted by cardiovascular diseases, this greatly limits the use of mice to model human cardiovascular diseases.⁵

A cardiovascular disease for which few pig models currently exist is congenital heart disease (CHD). CHDs are birth defects involving structural heart defects with abnormal cardiovascular anatomy. Although CHD models are readily available in mice, a major limitation of mice is their small size, which precludes the surgical intervention required for postnatal survival. Thus, analysis of mouse CHD models is restricted to examining the embryos or fetuses with CHD up to term. A second limitation is the different cardiac physiology mentioned above. However, although the cardiac physiology postnatally in mice and human differs markedly, they are comparable during embryonic/fetal development, with mice and human embryos/fetuses exhibiting similar heart rates. With the production of pig models of CHD, it would be possible to provide training for cardiac surgeons,

test new surgical procedures for CHD repair, test and develop ventricular assist devices for infants and pediatric subjects, or pilot new procedures for heart organ transplantation. Moreover, with availability of pig models of CHD, it will be possible to investigate different parameters that may impact the long-term outcome of patients with CHD.

Thus, having CHD models in pigs would be invaluable, but this requires a baseline knowledge of the normal developmental profile of the cardiovascular system in the pig embryo. Although detailed anatomical atlases of both human and mouse heart development have been published, with histological sections used to delineate heart structure across developmental stages, to our knowledge such an atlas has not been constructed for heart development in the pig. To this end, this study profiled pig heart development at both early and late time points by using a combination of magnetic resonance imaging (MRI), necropsy, and episcopic confocal microscopy for histological reconstructions.⁶ The resulting data set provides the first developmental atlas of the pig heart from early development to birth. Furthermore, examples of CHD in a CRISPR mutant pig show the feasibility of modeling CHD in the pig.

METHODS

The authors declare that all supporting data are available within the article (and its online supplementary files).

Animals

The pigs in this study were large white domestic crossbred animals (*Sus scrofa*). All animal work was humanely conducted under an approved University of Missouri Institutional Animal Care and Use Committee protocol. For wild-type samples, both fetuses and newborns analyzed in this study were generated by Landrace Large White cross parent gilt with semen from Choice USA Genetics (Choice USA, West Des Moines, IA). All pigs used for this study were from an approved farm facility and then moved into a University of Missouri animal facility for sample collection. All facilities are approved for biomedical pigs by the University of Missouri Animal Care and Use Committee and followed the *Guide for the Care and Use of Laboratory Animals*.

In Vivo Fetal Collections

Wild-type gilts were bred by artificial insemination with wild-type semen, with day 0 of gestation being classified as the first day of detectable estrus. Pregnant pigs were humanely euthanized on day 20, 26, 30, 35, 42, or 105 of gestation. The uterus was

opened on the antimesometrial side, and fetuses were removed. The whole fetus from each stage was then fixed in 4% paraformaldehyde at room temperature. For the day 42 fetus, the side of each fetus was sliced with a scalpel to allow fixative to permeate the chest cavity. For the day 105 fetus and newborn piglets, the heart and lungs were removed and placed in fixative.

Embryos were fixed in 4% paraformaldehyde or 10% formalin for 2 to 5 days. Three embryos per stage were analyzed, and for day 105 and newborn pigs, 5 animals were analyzed. Embryos at day 20 to 42 were necropsied by using a stereomicroscope, with digital images captured by using the Kontron Progres digital camera. MRI scans were conducted, followed by histological reconstructions, by using episcopic confocal microscopy. Fetuses at day 105 and newborn pigs at day 115 were analyzed by gross dissections.

Magnetic Resonance Imaging

Embryos to be MRI scanned were stained with gadolinium-based contrast agent to shorten the tissue T_1 . Well-fixed porcine embryos were immersed in 1:200 MultiHance (gadobenate dimeglumine; 529 mg/mL; Bracco Diagnostic, Inc, Monroe Twp, NJ) diluted with PBS at 4°C for 48 hours. After staining, the embryos were secured on a tongue depressor (McKesson Medical-Surgical, Irving, TX) with Webglue surgical adhesive (n-butyl cyanoacrylate; Patterson Veterinary, Devens, MA). The embryos were then immersed in Fomblin Y (perfluoropolyether; Sigma-Aldrich Millipore) to eliminate the susceptibility artifact at the tissue-air interface and to avoid dehydration during imaging.

MRI was performed on a Bruker Biospec 7T/30 system (Bruker Biospin MRI, Billerica, MA) with a 35-mm quadrature coil for both transmission and reception. Three-dimensional MRI was acquired with a fast spin echo sequence, the rapid acquisition with refocusing echoes, with the following parameters: effective echo time, 24.69 ms; rapid acquisition with refocusing echoes factor 8; and repetition time, 900 ms. The field of view, acquisition matrix, and voxel sizes varied on the basis of the embryo sizes. The typical spatial resolution for day 26, 30, and 35 embryos ranged from 39 to 46 mm, whereas that of day 42 embryos ranged from 45 to 62 mm. The 3-dimensional MRI imaging stacks were exported with DICOM format and could be reoriented to any viewing angles with Horos (horosproject.org).

Gross Dissections of the Heart

Because pigs are quadrupeds, some structures, which in bipedal mammals, such as humans, are

described as superior (superior caval vein) would be referred to as anterior or cranial in the pig, such as anterior caval vein. However, to better align the pig to the bipedal mammal, we have chosen, like others, to describe the hearts of pigs as in the bipedal mammals.⁷ Gross dissections were conducted for the day 105 and 115 pig samples following the direction of blood flow. First, the superior caval vein was identified and opened into the inferior caval vein. Then, the right-sided ventricle was opened from the right atrium through the atrioventricular valve (tricuspid) along the posterior wall near the septum to the apex. The incisions were then extended from the apex along the anterior wall next to the septum and through the outflow tract and pulmonary valve into the pulmonary trunk. The left atrial appendages were opened, and 2 pulmonary vein orifices were identified. The left ventricles were opened through the atrioventricular valve (mitral) along the posterior aspect near the septum to the apex, dividing the papillary muscles. The incisions were extended from the left ventricular apex along the anterior wall near the ventricular septum, then across the aortic valve, and the coronary arterial orifices were identified. The incision was then continued underneath the pulmonary trunk, extending around the aortic arch and into the thoracic aorta.

Structures of the heart were evaluated by using the sequential segmental analytic method, with each segment of the heart analyzed in turn starting with the atrial segment (right and left), then proceeding to the ventricles (right and left) and finally the arterial segment (aorta and pulmonary arteries). Each segment was identified by its least variable structures, not by variable features that can be altered in congenitally malformed hearts (such as connections between the segments, position in space of the segments, and thicknesses of their ventricular walls⁷⁻⁹).

Histopathology With Episcopic Confocal Microscopy

For embryos at day 20, 26, 30, and 35 after necropsy, the fetal pig hearts were embedded in paraffin for episcopic confocal microscopy. This entailed sectioning the paraffin-embedded sample by using a Leica SM2500 sledge microtome, and serial confocal images of the block face were captured using a Leica LSI scanning confocal microscope mounted above the sample block. The 2-dimensional serial image stacks collected are perfectly registered and were visualized by using the OsiriX Dicom viewer.¹⁰ The image stacks were further digitally resectioned in different imaging planes and 3-dimensional reconstructed for optimal viewing of different heart structures.

Guide RNA Design and In Vitro Transcription of Single Guide RNAs

One guide RNA, guide 1309 (GCTGCACAACACTT ACCAAC), was designed to target the end of exon 10 into the downstream intron of porcine *SAP130*. A T7 promoter sequence was added upstream of the 20-bp guide, and a gBlock was synthesized to use as template DNA in a manner similar as previously described.¹¹ *SAP130* guide 1309 RNA along with Cas9 RNA (TriLink Biotechnologies) were mixed for a final concentration of 20 ng/μL of Cas9 RNA and 10 ng/μL of guide RNA.

Oocyte Injection, In Vitro Fertilization, and Embryo Transfer

Mature oocytes were selected, and the guide RNA+Cas9 RNA were coinjected into the oocyte cytoplasm by using a FemtoJet microinjector (Eppendorf, Hamburg, Germany). The oocytes used for zygote injections are from large white domestic crossbred pigs obtained from a local Missouri abattoir and are of an unknown genetic background. After injection, oocytes were in vitro fertilized, as previously described, and cultured until day 4 to day 6 after fertilization.² At that time, morula and/or blastocysts were selected to be transferred into a recipient sow. Nine embryo transfers were completed. Semen used for in vitro fertilization is from large white domestic crossbred boars derived from Choice USA Genetics (Choice USA, West Des Moines, IA).

Polymerase Chain Reaction Screening for Insertions and Deletions

Deletions were determined by polymerase chain reaction (PCR) amplification of *SAP130* flanking a projected cutting site introduced by the CRISPR/Cas9 system. The forward primer (AAAACGATCTTC AGTACGGGCACA) and reverse primer (GCCTGGAA GAAATTTTTGGATGGT) amplify an 894-bp wild-type amplicon. For genotyping the piglets once born, the resulting PCR products were purified and sequenced by Sanger sequencing. The PCR product was also TOPO cloned into the pCR4 vector (Invitrogen) and transformed into chemically competent One Shot TOP10 *Escherichia coli* (Invitrogen). Plasmids from individual colonies were sequenced by Sanger sequencing to confirm the genotypes. All gene editing experiments were approved by the Institutional Biosafety Committee.

CRISPR Gene Edited *SAP130* Pigs

Nine embryo transfers resulted in 1 day 35 fetus collection and 2 litters of piglets born. Litter 24 had 7 piglets born alive, and those data will be reported herein. Piglets 1, 2, 3, and 4 contained *SAP130* monoallelic

edits, piglets 6 and 7 contained *SAP130* biallelic null edits, and piglet 5 contained 3 *SAP130* null alleles. Each of the 3 *SAP130* null piglets (5, 6, and 7) were born with anal atresia and failure to thrive, and were subsequently euthanized. A slice of tail was excised from tail docking of each piglet, and fibroblast cells were propagated as previously described.¹²

Fibroblast cells from the *SAP130* targeted pigs were analyzed for evidence of exon 10 skipping with analysis of cDNA generated from RNA isolated from pig fibroblast cells by using RNeasy mini kit with on-column DNase I digestion (Qiagen).¹³ RNA was converted to cDNA using a high-capacity RNA-to-cDNA kit (Applied Biosystems). For splicing analysis, PCR on the resulting cDNA was performed by using GoTaq DNA Polymerase and the following primers: forward, tccaccatctgcagcaatta; and reverse, attgtcgaatggtgacaca. The PCR product was then gel purified and sequenced.

Statistical Analysis

Our manuscript is an observational study and as such there are no statistics applied and no statistical analysis included.

RESULTS

Development of the embryonic and fetal pig heart was examined from the looped heart tube stage at day 20 after conception to term at day 115. Seven stages were examined, encompassing days 20, 26, 30, 35, 42, 105, and 115. For the earlier stages, comprising up to day 42, external cardiac anatomy was examined by conducting necropsy with a stereomicroscope. This was followed by cardiac MRI examination (except for day 20 embryos), and then episcopic confocal histological 3-dimensional reconstructions (except for day 42). The MRI and episcopic confocal microscopy analyses provided visualization of intracardiac anatomy. For fetuses at day 105 and 115, MRI analysis and images from gross dissections provided visualization of intracardiac anatomy.

Gross Developmental Profile of Pig Embryogenesis From Day 20 to Day 42

The looped heart tube in the day 20 embryo shows distinct primitive right and left ventricles (Figure 1A and 1B). Only a single outflow was present, connected to the right ventricle (Figure 1B). The forelimb buds and >20 somites can be observed. The hindlimb bud is just appearing as a small protrusion caudally. The first and second pharyngeal arches are evident, and neural tube closure is complete with formation of the primitive brain ventricles. Also evident are the optic and otic vesicles.

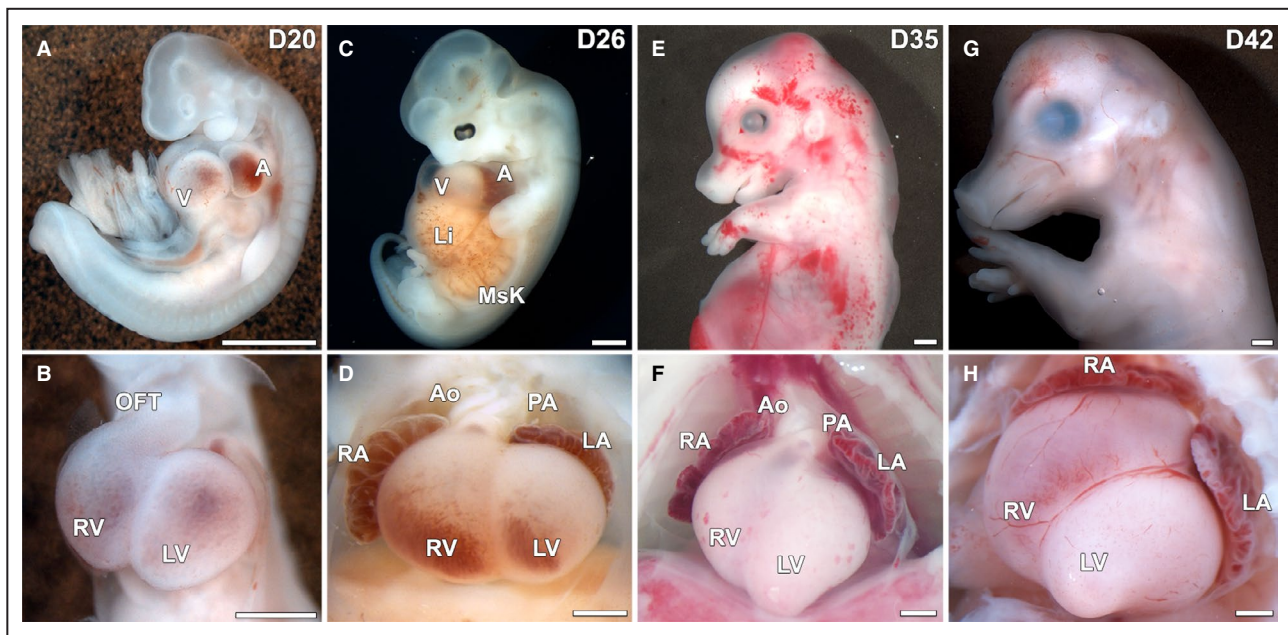


Figure 1. Pig embryo development from day 20 (D20) to day 42 (D42).

A, Sagittal view of the D20 pig embryo. **B**, Frontal view of the D20 pig heart, showing a common outflow tract (OFT) arising from the right ventricle (RV). **C**, Sagittal view of the day 26 (D26) pig embryo, showing relative position of the atria (A), ventricle (V), liver (Li), and mesonephric kidney (MsK). **D**, Frontal view of the D26 pig heart, showing separate aorta (Ao) and pulmonary artery (PA) and enlargement of all 4 heart chambers. **E**, Sagittal view of the day 35 (D35) pig embryo. Bar=2 mm. **F**, Frontal view of the D35 pig heart, showing continued rotation of the heart to mesocardia positioning. **G**, Sagittal view of the D42 pig embryo. **H**, Frontal view of the D42 pig heart. **A** through **H**, Images displayed are photographs collected by necropsy of wild-type pig embryos ranging from D20 to D42 in development. LA indicates left atrium; LV, left ventricle; and RA, right atrium.

By day 26, significant embryo development and growth have occurred, with the liver and mesonephric kidneys prominently observed (Figure 1C). Extended forelimb and hindlimb paddles are present, and the tail has formed caudally. The eye now shows distinct pigmentation. The forebrain, midbrain, and hindbrain are well delineated, and the frontonasal process is forming. At this stage, septation of the outflow tract is evident, with 2 distinct great arteries observed: the pulmonary artery and the aorta (Figure 1D).

By day 35, craniofacial and limb development has advanced considerably, with the eye, pina, and snout all well formed. Distinct upper and lower jaws are evident (Figure 1E). Formation of digits in the limb is evident. The heart has undergone rotation such that the left ventricle forms a clear apex pointing toward the body's midline (Figure 1F).

On day 42, the fetal pig appeared anatomically similar to that of the day 35 pig but significantly larger (Figure 1G and 1H). Distinct remodeling of the craniofacial structures and autopod of the limb provides the pig embryo with distinct features that are characteristic of the pig (Figure 1G and 1H). Thus, remodeling of the frontonasal process has created a pointed snout, and the limb autopod now has the appearance of hoofs. At this stage, external whole mount views of the heart show little change.

Dynamic Development of the Cardiovascular System

By using episcopic confocal microscopy, we constructed a profile of the dynamic development of the pig heart from day 20 to day 42, when major events in cardiac morphogenesis are completed. At day 20, an undivided or common outflow tract is observed, positioned over the primary interventricular foramen (Figure 2A and Video S1 and S2). Atrioventricular cushions are observed, forming a primitive common atrioventricular valve (Figure 2B and 2C). It is positioned mostly over the primitive left ventricle and plays an important role in regulating blood flow between the atria and undivided common ventricles (Figure 2A). Atrial septation has been initiated with formation of the primary septum or septum primum (Figure 2B). At this stage, the ventricular myocardium has not undergone compaction, and there is only a single outflow tract emerging from the right ventricle (Figure 2D and 2E and Video S3). Transverse views of the outflow tract cushions showed no evidence of septation proximally or more distally (Figure 2F and 2G and Video S3). At day 26, the outflow tract has undergone septation to form the aorta and the pulmonary artery (Figure 3A and Video S4). The atrioventricular cushions have remodeled, forming the 3-leaflet tricuspid valve between the

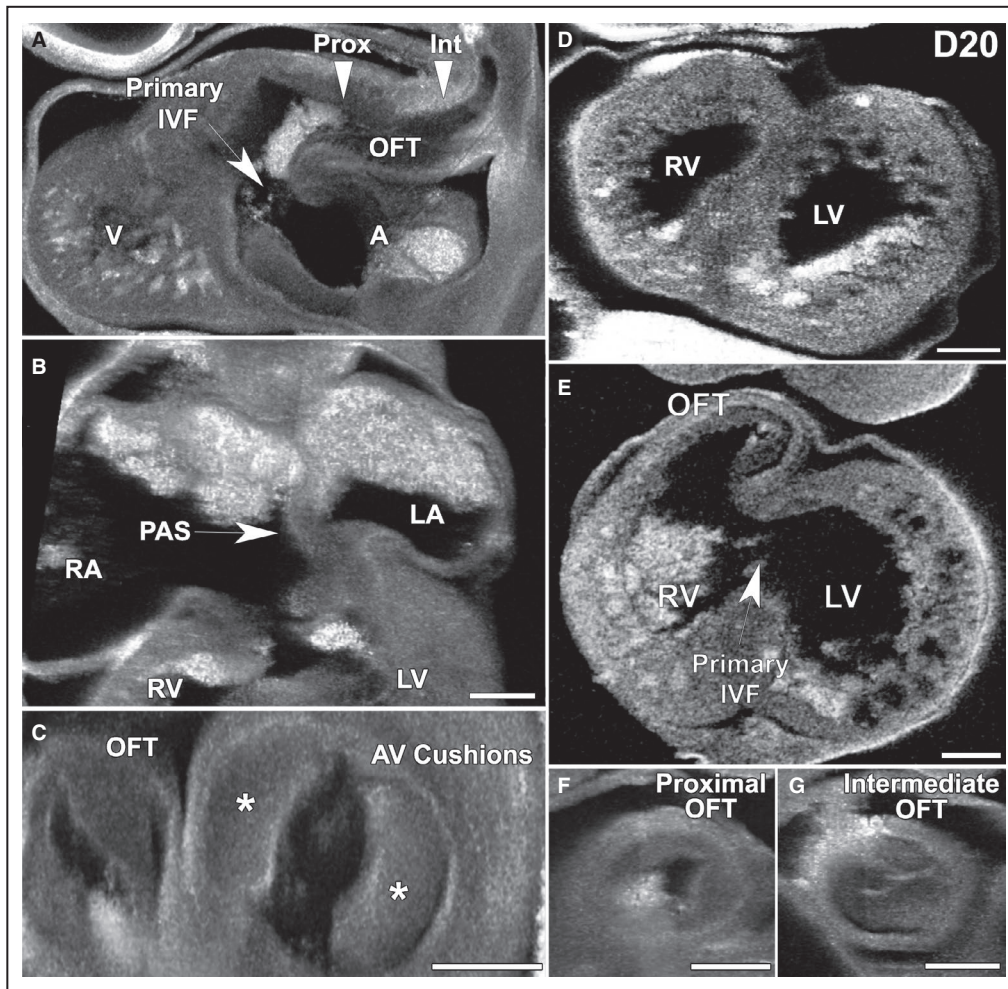


Figure 2. Anatomy of the pig heart at day 20 of gestation.

A, Sagittal view of the heart, showing positioning of the outflow tract (OFT) and atrium (A) over the primary interventricular foramen (IVF). Arrowheads delineate proximal and intermediate regions of the developing OFT. **B**, Frontal view of the developing atrial segment of the heart reveals a common atrial valve over the left ventricle (LV) with left and right atria separated by the primary atrial septum (PAS). **C**, Transverse sections through the atria reveal atrioventricular (AV) cushions (* denotes AV cushion tissue). **D**, Transverse sections through the ventricles (Vs) reveal ventricular myocardial noncompaction. **E**, A frontal view of the heart shows a common OFT exiting the right ventricle (RV). **F** and **G**, The OFT cushion at proximal (Prox; **F**) and intermediate (Int; **G**) locations shows a single OFT without evidence of septation. **A** through **G**, Images displayed were collected by episcopic confocal microscopy. LA indicates left atrium; and RA, right atrium.

right atrium and right ventricle, and the 2-leaflet mitral valve between the left atrium and left ventricle. These valves are thick at this stage (Figure 3B). Invagination seen at the roof of the atria reflects initiation in formation of the secondary atrial septum or septum secundum (Figure 3B and Video S4). Ventricular compaction has begun with a thin layer of compact myocardium detected (Figure 3C and Videos S5 and S6). The aortic and pulmonary valves are formed, each with 3 distinct leaflets. As observed with the atrioventricular valves, these outflow valves are thick at this stage (Figure 3D and 3E).

At day 30, the heart has undergone significant maturation, with prominent compaction of the

ventricular myocardium observed in both the right and left ventricles (Figure 4A and Videos S7, S8, and S9). The tricuspid and mitral valves have undergone remodeling and are thinner than at day 26 (Figure 4B). Cross-sections of the aorta and pulmonary valves show well-formed 3-leaflet valves, although they remain thickened (Figure 4C,D). The atrioventricular and the outflow semilunar valves continue to remodel as the heart develops, with further thinning observed in the day 35 (Figure 4E through 4G) and day 42 embryos (see MRI data in Videos S10–S12). Completion of atrial septation is observed between day 35 and day 40 with emergence of the recessed oval fossa

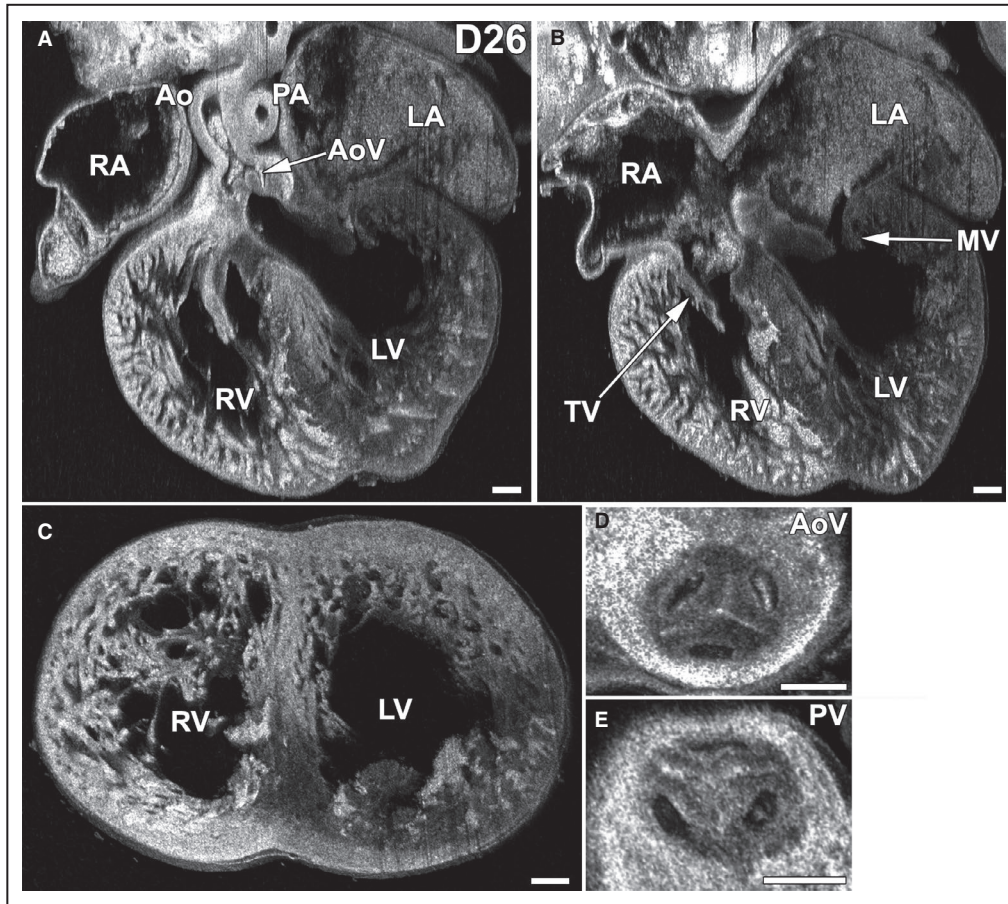


Figure 3. Anatomy of the pig heart at day 26 (D26) of gestation.

A, Four-chamber view of the heart shows aorta (Ao) arising from the left ventricle (LV). **B**, Four-chamber view of the heart revealing a developing tricuspid valve (TV) and a developing mitral valve (MV). Also visible is a characteristic infolding at the roof of the atrium. **C**, Transverse view of the ventricular segment of the heart reveals thin compact myocardium beginning to form. **D**, View of the aortic valve and **E**, view of the pulmonary valve, each showing three leaflets. **A** through **E**, Images displayed were collected by episcopic confocal microscopy. AoV indicates aortic valve; LA, left atrium; PA, pulmonary artery; PV, pulmonary valve; RA, right atrium; and RV, right ventricle.

with growth of the septum primum and secundum (Figure S1).

Development of the coronary arteries was also noted. Emergence of coronary vessels is evident at day 26. This can be observed at the base of the aorta (Figure S1A), and along the epicardial surface of the heart (Figure S1B). Coronary artery insertion into the aorta is observed at day 30, after initiation of ventricular compaction (Figure S2C through S2E).

Cardiac Anatomy of the Neonatal Pig

Necropsies were performed on the thoracic-abdominal viscera in the neonatal pigs. The position of the heart within the chest, direction of the cardiac apex, configuration of the heart, appearance of the atrial appendages, and the morphology and relationship of the great vessels and veins were examined. The pig

heart, including its apex, was located on the midline. The heart has been described as having a “valentine” shape (Figure 5A), with apex formed by the left ventricle (Figure 5B and 5C).⁷ After the thoracic-abdominal organs were removed en block to preserve vascular connections, the cardiovascular connections, both arterial and venous, were evaluated. The heart/lung along with the great arteries and thoracic aortas were removed as a unit, and the heart was analyzed by gross dissection by using a segmental approach following the direction of blood flow (see Methods).

Atrial Segment

The right atrial appendage has a tubular appearance, as previously reported, with the left atrial appendage comparable in size to the right, but with a somewhat triangular shape (Figure 5D and 5E).¹⁴ The inferior caval

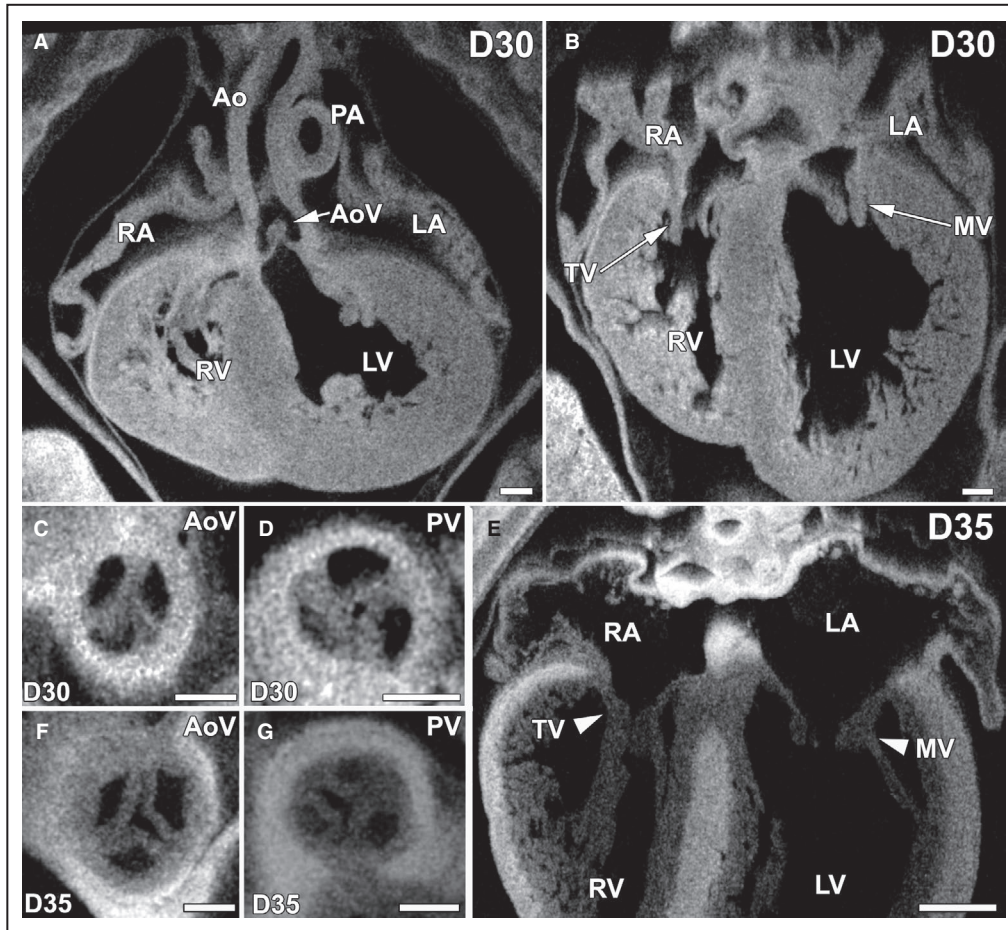


Figure 4. Anatomy of the pig heart at day 30 (D30) and day 35 (D35) of gestation.

A, Four-chamber view of the heart shows aorta (Ao) arising from the left ventricle (LV) at D30. **B**, Four-chamber view of the heart reveals continued development and remodeling of the tricuspid valve (TV) and mitral valve (MV) at D30. **C** and **D**, Transverse views through the developing aortic valve (AoV; **C**) and pulmonary valve (PV; **D**) show each valve has 3 cusps that have begun to remodel but remain thickened at D30. **E**, Four-chamber view of the D35 pig heart reveals thinner TV and MV. **F** and **G**, Transverse views through the AoV (**F**) and PV (**G**) of the D35 pig heart. **A** through **G**, Images displayed were collected by episcopic confocal microscopy. LA indicates left atrium; PA, pulmonary artery; RA, right atrium; and RV, right ventricle.

vein was not directly in line with the superior caval vein but connected to the right atrium almost at a right angle to the superior caval vein (Figure 5F). In addition, the left azygous vein drained into the coronary sinus, which is a left heart structure connected to the right atrium near the inferior caval vein orifice (Figure 5G).⁷ The aorta and pulmonary artery exhibit a configuration similar to humans, and at the newborn stage an arterial duct was still visible (Figure 5H). Dissection of the superior caval vein showed it opening into the right atrium at a right angle to the inferior caval vein (Figure 6A). The terminal crest along with the configuration of pectinate muscles were identified, confirming it is a morphologic right atrium (Figure 6A). In addition, the oval fossa was visible and had a recessed appearance (Figure 6A). In contrast, the morphologic left atrium lacked a terminal crest, consistent with left ventricular identity (Figure 6B).

Ventricular Segment

The right ventricle of the pig showed coarse trabeculations over the entire septal surface, and the tricuspid valve had tendinous cords that were attached to the septal surface (Figure 6C). The pulmonary valve was supported by and separated from the tricuspid valve by a muscular sleeve. The moderator band was easily identifiable in the right ventricle attached to the septomarginal trabeculations at a high position in the outflow tracts (Figure 6D). The pulmonary trunk exited the right ventricle, then gave rise to a single pulmonary, which immediately branches into the 2 distinct pulmonary arteries (Figure 6E).

In contrast to the tricuspid valve, the mitral valve was identified within the left ventricle with tendinous cords attached to the papillary muscles. The cords were not attached directly to the ventricular septal surface. The

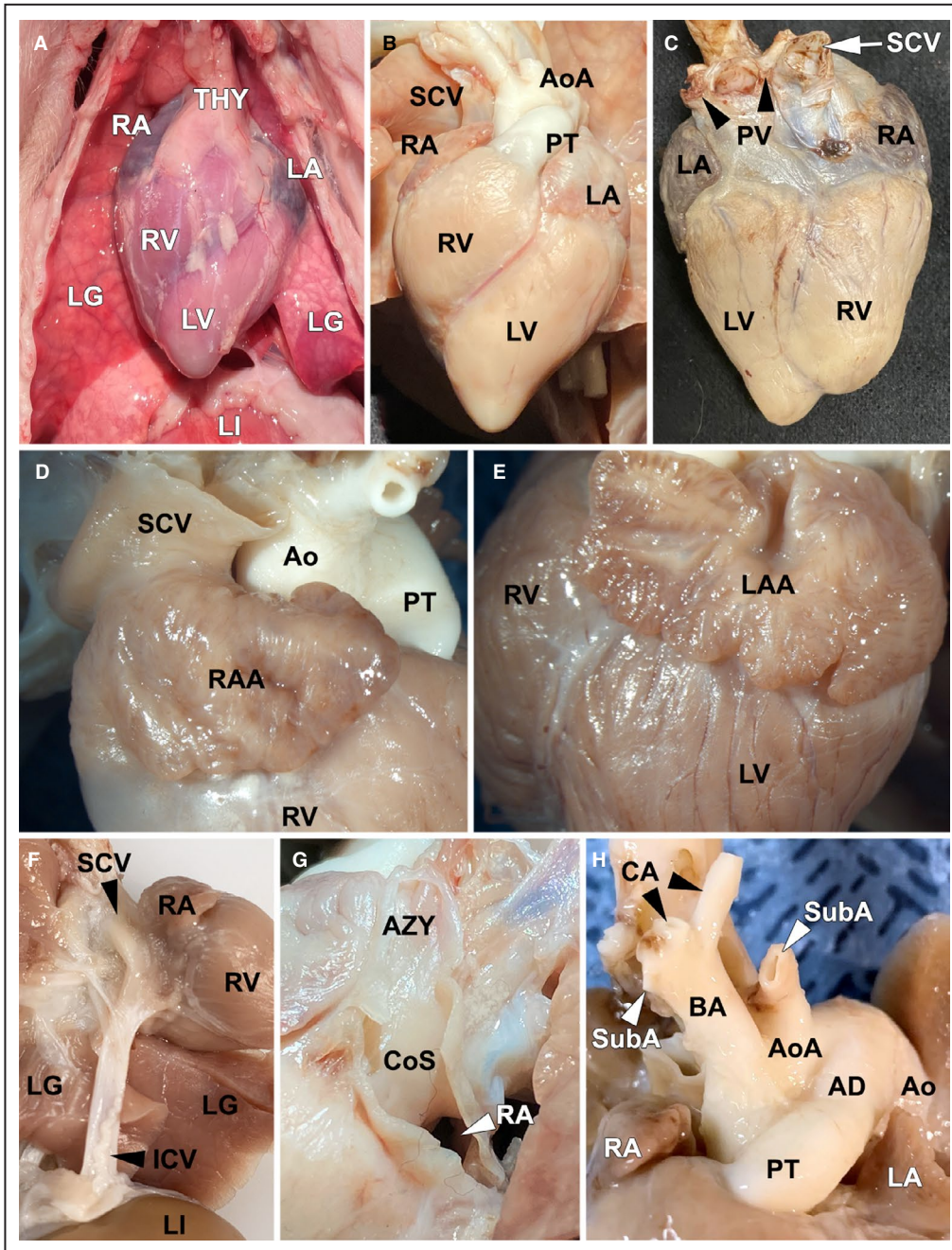


Figure 5. External gross anatomy of the pig heart at 105 to 115 (term) days gestation age.

A, In situ image, showing the normal central position of the heart and ventricular apex. **B**, Anterior aspect of the heart. **C**, Posterior aspect of the heart. **D**, Right atrial appendage (RAA). **E**, Left atrial appendage (LAA). **F**, Caval veins. **G**, Opened coronary sinus with left azygous vein. **H**, Great arteries of the heart. AD indicates arterial duct; Ao, aorta; AoA, aortic arch; AZY, left azygous vein; BA, brachiocephalic artery; CA, carotid artery; CoS, coronary sinus; ICV, inferior caval vein; LA, left atrium; LG, lung; LI, liver; LV, left ventricle; PT, pulmonary trunk; PV, pulmonary vein; RA, right atrium; RV, right ventricle; SCV, superior caval vein; SubA, subclavian artery; and THY, thymus gland.

mitral valve was in fibrous continuity with the aortic valve, and the subarterial surface was smooth, with the apical components showing course trabeculations (Figure 6F and 6G). The aorta exited the left ventricle posterior to

the pulmonary artery and gave rise to the right and left coronary arteries (Figure 6H). The left coronary artery further divided into the left anterior descending and the circumflex coronary arteries (Figure 6H).

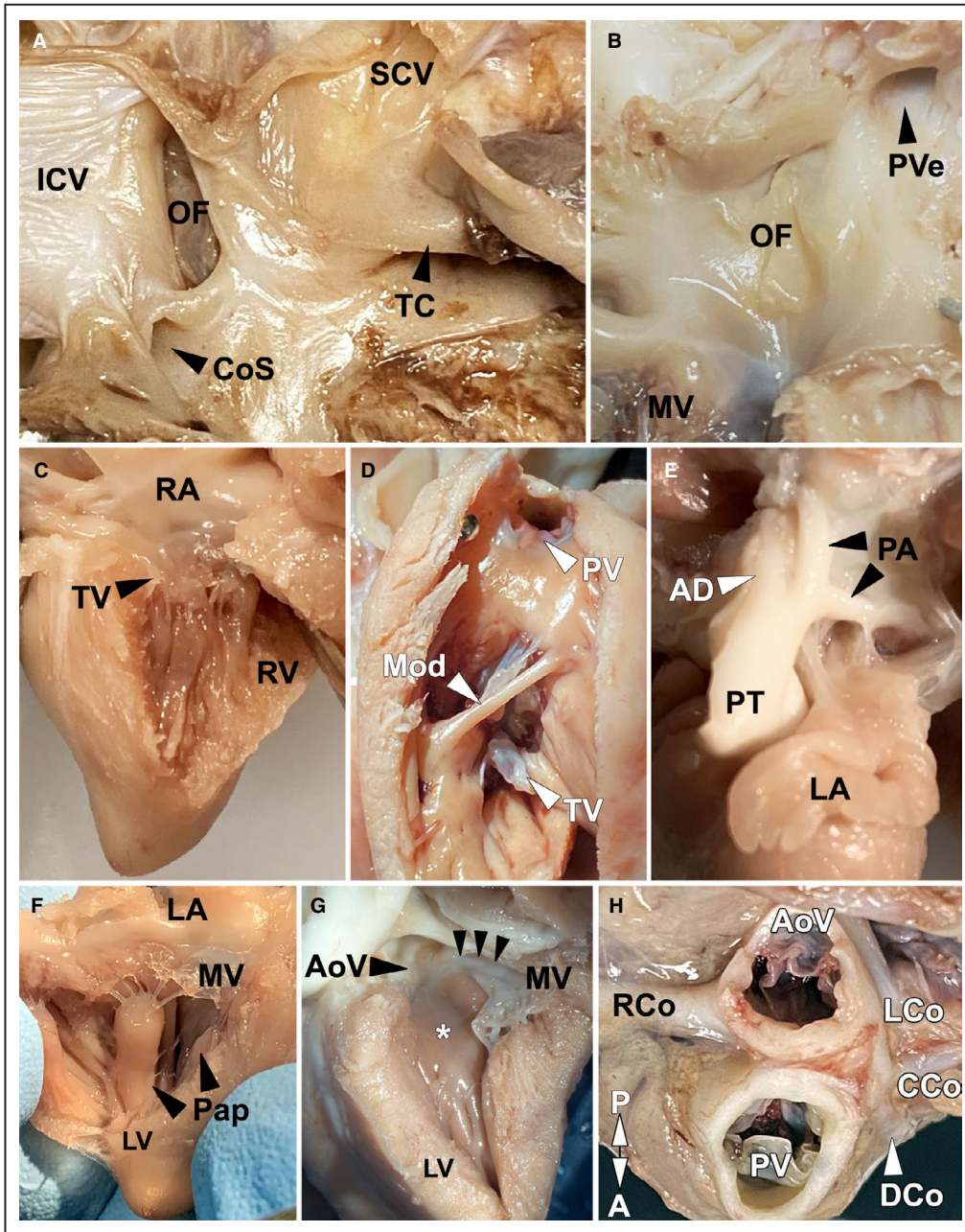


Figure 6. Internal gross anatomy of the pig heart at 105 to 115 (term) days gestation age. **A**, Right atrial septum. **B**, Left atrial septum. **C**, Septal surface of the right ventricle (RV). **D**, Right ventricular outflow tract. **E**, Pulmonary arteries (PAs). **F**, Inlet left ventricle (LV)/mitral valve (MV). **G**, Septal surface of the LV. **H**, Base of heart, showing coronary arteries. The * indicates smooth subarterial surface of the LV; and black arrowheads, fibrous continuity between aortic valve (AoV) and MV. AD indicates arterial duct; CCo, circumflex coronary artery; CoS, coronary sinus; DCo, left descending coronary artery; ICV, inferior caval vein; LA, left atrium; LCo, left coronary artery; Mod, moderator band; OF, oval fossa; Pap, papillary muscle; PT, pulmonary trunk; PV, pulmonary vein; PVe, pulmonary vein; RA, right atrium; RCo, right coronary artery; SCV, superior caval vein; TC, terminal crest; and TV, tricuspid valve.

Arterial Segment and Branches

The arterial segment consisted of a pulmonary trunk, right and left pulmonary arteries, arterial duct, coronary arteries, ascending aorta and aortic arch,

brachiocephalic artery, carotid and subclavian arteries, and thoracic aorta. The pulmonary and systemic great arteries were distinguished from each other by their branching patterns. In the pig, the pulmonary trunk gave

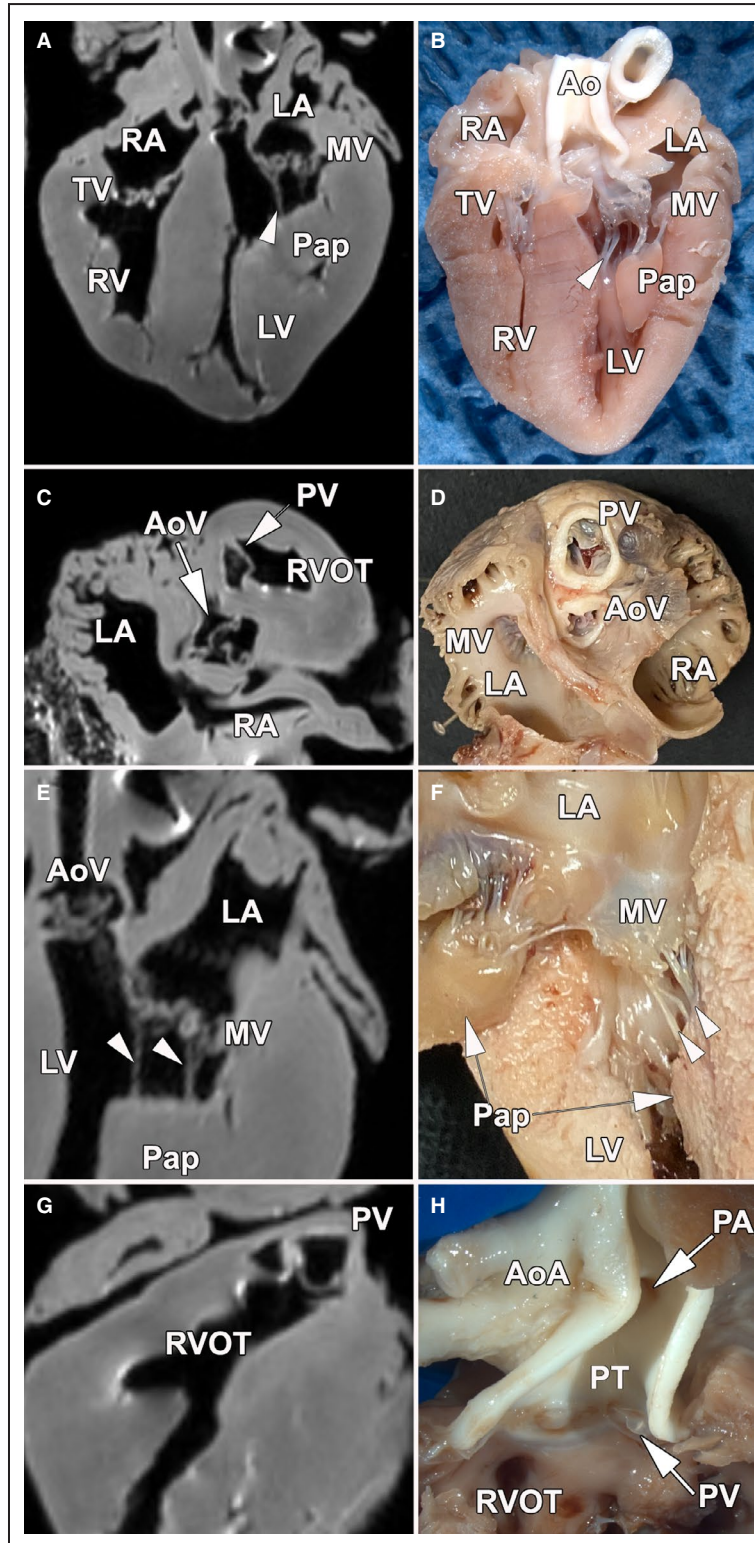


Figure 7. Cardiac magnetic resonance imaging-gross anatomy comparisons of newborn pig heart.

A and B, Four-chamber views. **C and D,** Base views. **E and F,** Mitral valve (MV). **G and H,** Pulmonary outlet. White arrowheads indicate tendinous cords. Ao indicates aorta; AoA, aortic arch; AoV, aortic valve; LA, left atrium; LV, left ventricle; PA, pulmonary artery; Pap, papillary muscle; PT, pulmonary trunk; PV, pulmonary valve; RA, right atrium; RV, right ventricle; RVOT, right ventricular outlet tract; and TV, tricuspid valve.

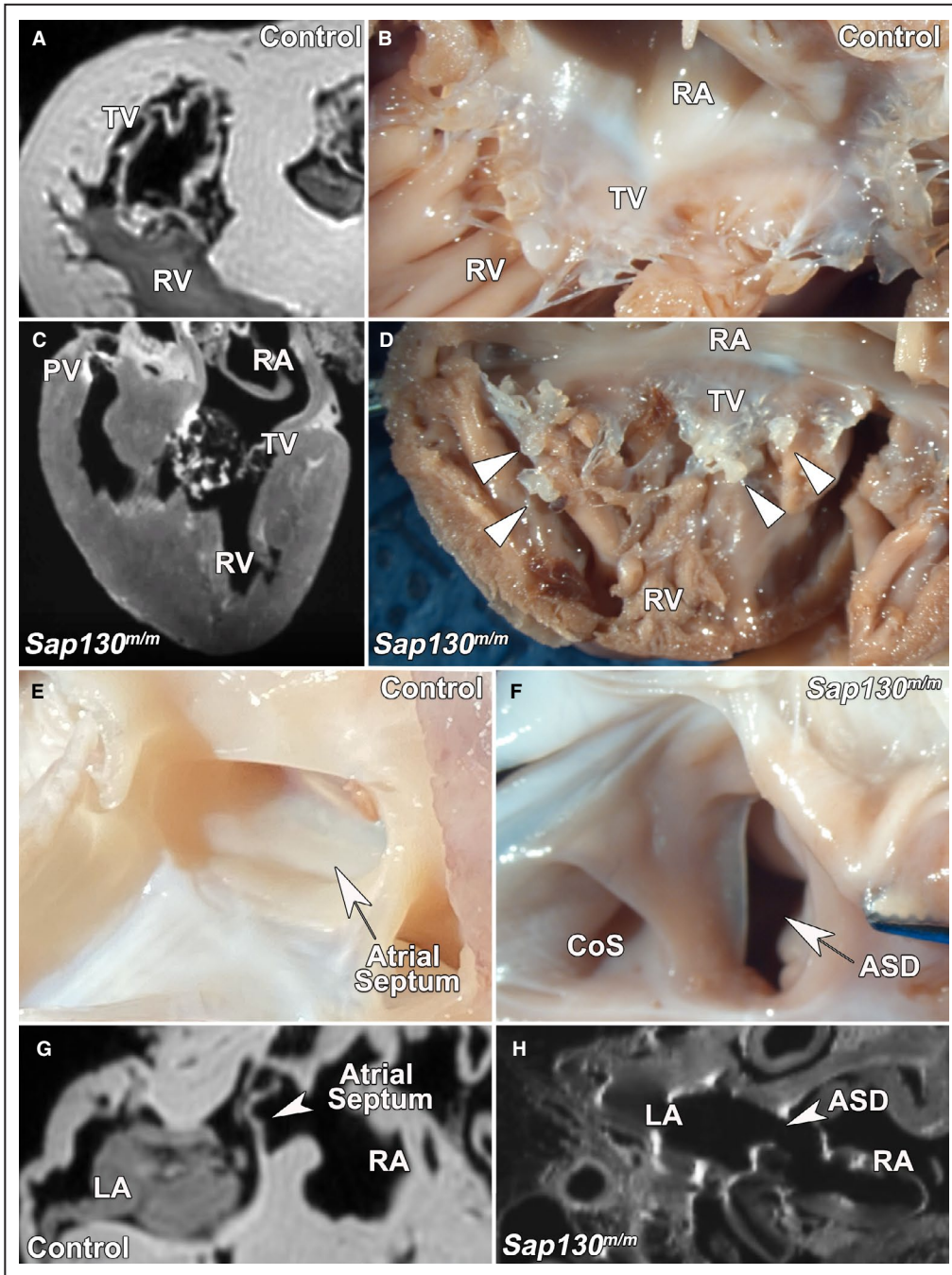


Figure 8. Magnetic resonance imaging (MRI) and gross findings of cardiac malformations in 3 term pigs.

A and **B**, Normal tricuspid valve (TV) morphology on MRI (**A**) and necropsy (**B**) found in a wild-type newborn pig. **C** and **D**, Dysplastic TV found in a *SAP130* gene edited pig by MRI (**C**) and necropsy (**D**). **E** and **F**, Wild-type newborn pigs showed intact atrial septum on necropsy (**E**), whereas one *SAP130* gene edited pig showed an oval fossa atrial septal defect (ASD), as viewed from the right atrium (RA; **F**) in addition to TV dysplasia. **G** and **H**, The atrial septum can also be identified in wild-type newborn pig by MRI (**G**), whereas the *SAP130* gene edited pig shows an ASD (**H**). CoS indicates coronary sinus; LA, left atrium; PV, pulmonary valve; and RV, right ventricle.

rise to a single pulmonary artery that quickly divided into right and left pulmonary arteries (Figure 6E), and the aortic arch, which was left sided, gave rise to the brachiocephalic and left subclavian arteries (Figure 5H).

MRI Analysis of Cardiac Anatomy in the Newborn Pig

MRI of the newborn pig heart provided comparable findings to those observed by gross dissections. In

the 4-chamber view, tricuspid and mitral valves and papillary muscles can be seen, similar to gross dissections of the heart (Figure 7A and 7B and Video S13). Digitally reslicing the MRI image stacks from the same pig heart in the transverse view showed views of the aortic and pulmonary valves, similar to those observed by gross dissections in a transverse plane (Figure 7C and 7D and Videos S14 and S15). MRI of the left ventricular outflow tract showed the aortic valve in fibrous continuity with the mitral valve. Tendinous cords connected the mitral valve to the papillary muscle of the left ventricle (Figure 7E). These tendinous cords are also visible in the gross dissections of the left ventricle (Figure 7F). Similar MRI analysis of the right ventricular outflow tract shows the pulmonary valve arising from the right ventricle, similar to the coronal gross dissection view of the right ventricle (Figure 7G and 7H).

Modeling CHDs in Pigs

Analysis of CRISPR gene targeted newborn pigs bearing splicing defect mutation in *SAP130*, a protein in the histone deacetylase repressor complex previously shown to contribute to hypoplastic left heart syndrome (HLHS), yielded CHD phenotypes.¹³ We observed 3 *SAP130* edited pigs (Figure S3) had tricuspid valve defects. In 2 newborn pigs, there was tricuspid valve dysplasia with a nodular appearance that can be observed in the MRI and with gross dissection when compared to control (Figure 8A,B versus C,D). One of these neonates also showed an oval fossa atrial

septal defect (Figure 8E through 8H). Interestingly, one *SAP130* edited fetus recovered at day 35 had already expired, showing a more severe phenotype comprising tricuspid atresia with complete failure of the tricuspid valve to form.

In addition, in the course of examining wild-type pig embryos for this study, one neonatal pig was observed to have a cardiac situs abnormality. This comprised dextrocardia, in which the heart was malrotated, with the heart apex pointing to the right side of the body, but the abdominal viscera were normally positioned (Figure 9). Further analysis by MRI showed no intracardiac defects. This suggests a possible role of a background mutation perturbing left-right patterning in the herd.

DISCUSSION

Our analysis of cardiovascular development in the pig showed major structures of the heart are formed by day 30, when all 4 chambers of the heart are present, and the atria, ventricle, and outflow tract have septated. The pig heart was found to follow a similar developmental course to the hearts of both human and mouse.¹⁵ Between the earliest stages we analyzed, day 20 and 26, the pig heart underwent atrial septation, and formation of the muscular ventricular septum (Figure 10). Also, at this stage, the outflow tract divided from a single vessel into the aorta and pulmonary artery. The outflow tract cushions also begin to form (Figure 10). These stages are comparable to embryonic day (E) E11.5 and E12.5 in mouse embryos

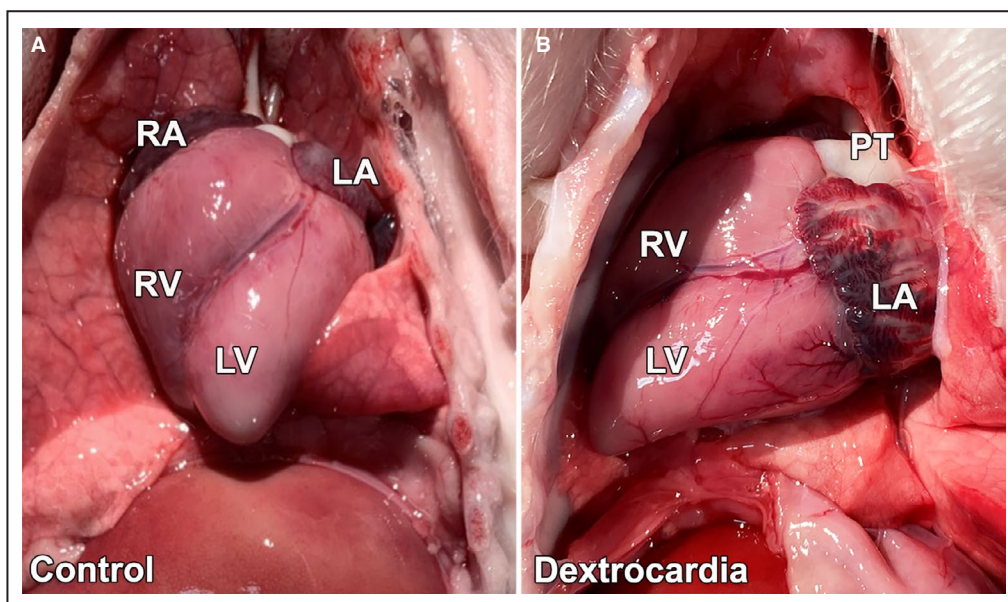


Figure 9. Dextrocardia in a newborn pig.

A and **B**, Necropsy view of the heart from a 2-day-old pig, showing normal cardiac positioning (**A**), whereas a second 2-day-old pig exhibits dextrocardia (**B**). LA indicates left atrium; LV, left ventricle; PT, pulmonary trunk; RA, right atrium; and RV, right ventricle.

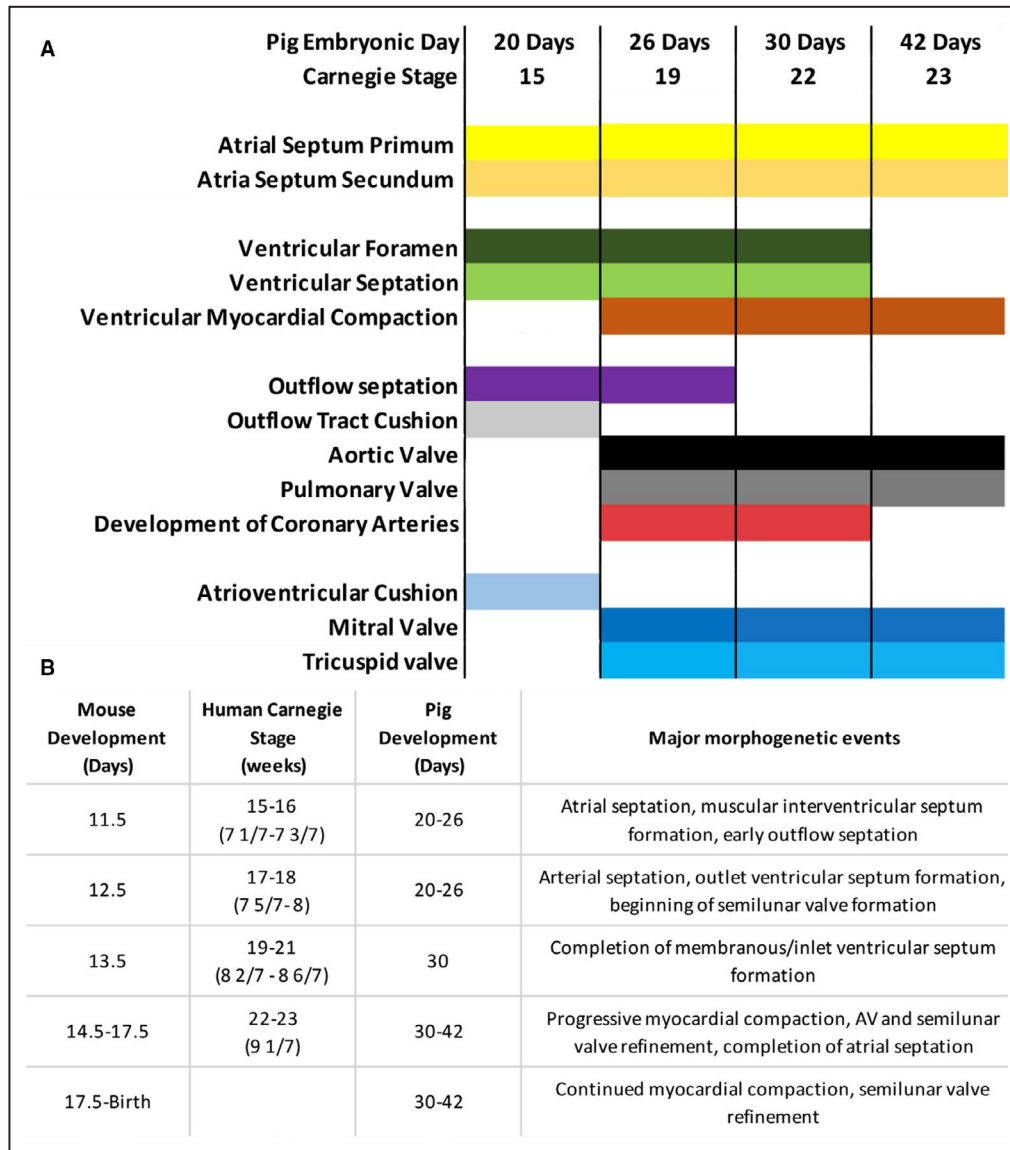


Figure 10. Pig heart developmental timeline and comparison to mouse and human.
A, Developmental profile of cardiac morphogenesis in the pig. **B**, Comparison of heart development between pig, mouse, and human.

and Carnegie stage 15 to 18 in the developing human fetus (Figure 10).^{15,16} By day 26, all major cardiac structures were identified in the fetal pig. By day 30, ventricular septum formation is complete, while compaction of the ventricular myocardium continues through at least day 42 (Figure 10). Between day 30 and 42, there is continued remodeling of the cardiac valves that will sculpt the thickened valves into the thin leaflets of mature cardiac valves. These developmental stages are comparable to E14.5 to birth in mouse embryos and Carnegie stages 19 to 23 of the developing human fetus (Figure 10B). Despite the overall similarities between pig and human heart development, there are some differences. For example, although the morphologic right ventricle is

distinctly different from the morphologic left ventricle in pig and human, in pigs the ventricular walls were thicker than that seen in the human heart. In the human heart, the apical component is typically used to determine if a ventricle is morphologically right or left, because the apical component of the right ventricle shows coarse trabeculations, and in the left ventricle the trabeculations are small and crisscrossing. However, in pigs, the apical trabeculations in both ventricles were coarse. Nevertheless, other structures can be used to determine if a ventricle is morphologically right or left, such as the type of atrioventricular valves (tricuspid or mitral), cordal attachments to septal surfaces as opposed to papillary muscles only, existence of a moderator band,

and presence of complete muscular outlets (sleeves) versus fibrous continuity between the atrioventricular valves and the arterial valves and smooth subarterial septal surfaces.

One of the newborn pigs examined exhibited dextrocardia, suggesting the presence of a background mutation in the herd causing laterality defects. Nevertheless, all the pig hearts examined, including the one with dextrocardia, had concordant atrioventricular and ventriculoarterial connections. Analysis of 3 gene edited pigs harboring a *SAP130* mutation generated by CRISPR gene editing revealed tricuspid dysplasia or atresia. Although this mutation was shown to cause HLHS in mice, HLHS was observed with incomplete penetrance and only in combination with a second mutation in *Pcdha9*.¹³ Efforts are currently underway to generate such a digenic pig to attempt to create an HLHS pig model. Overall, these findings show the feasibility of modeling CHD in pigs, with the main advantages being its size and cardiac physiology being similar to that of human.

Availability of pig models of CHD that can be maintained postnatally would provide a wealth of opportunities to pursue surgical and outcome studies. Currently, 30% of patients with HLHS experience heart failure and die within the first year of life, for which heart transplant is the ultimate therapy. Having a pig model of HLHS would allow investigations into the possible causes for such acute early heart failure. Also, pig models of CHD would provide the means to develop and test ventricular assist devices optimized for infants as a bridge to heart transplantation. Ventricular assist devices currently available have not been specifically developed for use in infants. A pig model of CHD, such as HLHS, would also provide invaluable opportunities for training surgeons in acquiring the surgical skills for congenital cardiac surgeries. The pig CHD model would also provide opportunities for testing new surgical procedures, conducting postsurgical outcome studies, or pursuing preclinical studies to test the efficacy of different therapies before conducting clinical trials in patients,^{17,18} such as the pursuit of stem cell therapy for HLHS.

Although our study was focused on the full-size pig, mini pigs would be another option. Although their smaller size is advantageous in terms of space and cost for animal housing, the mini pigs are more difficult to breed, and they have lower fecundity, with litter size of only 3 or 4 versus 15 to 18 in the full-size pig. Also, for developing human CHD models for surgical manipulations, newborn animals from the full-size pig are superior for modeling a newborn human infant. Using MRI, rapid noninvasive assessments can be conducted for CHD diagnosis even from early developmental stages (from day 30 and later).

Furthermore, full-sized pigs with the full range of body weight would allow investigations into the long-term physiological impact of CHD surgical palliation. With surgical advances, currently in the United States there are more adults with CHD than children born annually with CHD.¹⁹ With this rapidly increasing adult population with CHD has also come the appreciation of multiple long-term complications, such as those seen in patients with HLHS after the final post-Fontan surgical palliation.²⁰ With availability of full-size CHD pig models, the full range of hemodynamic loads similar to those seen in adults with CHD can be modeled and investigated. Overall, our study documenting the developmental profile of pig heart development will facilitate the future development of genetically engineered pig models of CHD for preclinical studies. Such pig models can help accelerate clinical translational studies that can improve outcomes for patients with CHD or other cardiovascular diseases.

ARTICLE INFORMATION

Received March 12, 2021; accepted May 14, 2021.

Affiliations

Department of Developmental Biology, University of Pittsburgh School of Medicine, Pittsburgh, PA (G.C.G., W.D., Y.W., C.W.L.); and Division of Animal Sciences, Animal Science Research Center, National Swine Resource and Research Center, University of Missouri, Columbia, MO (B.K.R., K.M.W., M.S., L.D.S., R.F.C., R.S.P., K.D.W.).

Acknowledgments

The University of Missouri would like to acknowledge Jason Dowell, Gina Farinella, Nathan Schwartz, Sabrina Hammond, and Skylar Young. This work could not be performed without their valuable contribution to pig care and sample collection.

Sources of Funding

This work is supported by funding for the National Swine Resource and Research Center (Drs Prather and Wells) from the National Institute of Allergy and Infectious Disease, the National Institute of Heart, Lung, and Blood, and the Office of the Director (U42OD011140), and grants HL142788 (Dr Lo) and HD097967 (G.C. Gabriel).

Disclosures

None.

Supplementary Material

Figures S1–S3
Supplementary Video Legends
Videos S1–S15

REFERENCES

1. Perleberg C, Kind A, Schnieke A. Genetically engineered pigs as models for human disease. *Dis Model Mech*. 2018;11:dmm030783. DOI: 10.1242/dmm.030783.
2. Redel BK, Prather RS. Meganucleases revolutionize the production of genetically engineered pigs for the study of human diseases. *Toxicol Pathol*. 2016;44:428–433. DOI: 10.1177/0192623315613160.
3. Shiels HA, White E. The frank-startling mechanism in vertebrate cardiac myocytes. *J Exp Biol*. 2008;211:2005–2013. DOI: 10.1242/jeb.003145.
4. Lillywhite HB, Zippel KC, Farrell AP. Resting and maximal heart rates in ectothermic vertebrates. *Comp Biochem Physiol A Mol Integr Physiol*. 1999;124:369–382. DOI: 10.1016/S1095-6433(99)00129-4.

5. Janssen PM, Biesiadecki BJ, Ziolo MT, Davis JP. The need for speed: mice, men, and myocardial kinetic reserve. *Circ Res*. 2016;119:418–421. DOI: 10.1161/CIRCRESAHA.116.309126.
6. Liu X, Kim AJ, Reynolds W, Wu Y, Lo CW. Phenotyping cardiac and structural birth defects in fetal and newborn mice. *Birth Defects Res*. 2017;109:778–790.
7. Devine WA, Debich DE, Anderson RH. Dissection of congenitally malformed hearts, with comments on the value of sequential segmental analysis. *Pediatr Pathol*. 1991;11:235–259. DOI: 10.3109/15513819109064762.
8. Anderson RH, Shirali G. Sequential segmental analysis. *Ann Pediatr Cardiol*. 2009;2:24–35. DOI: 10.4103/0974-2069.52803.
9. Praagh RV. The segmental approach to diagnosis in congenital heart disease. *Birth Defects: Original Article Series*. 1972;8:4–23.
10. Rosset A, Spadola L, Ratib O. Osirix: an open-source software for navigating in multidimensional dicom images. *J Digit Imaging*. 2004;17:205–216. DOI: 10.1007/s10278-004-1014-6.
11. Whitworth KM, Benne JA, Spate LD, Murphy SL, Samuel MS, Murphy CN, Richt JA, Walters E, Prather RS, Wells KD. Zygote injection of CRISPR/Cas9 RNA successfully modifies the target gene without delaying blastocyst development or altering the sex ratio in pigs. *Transgenic Res*. 2017;26:97–107. DOI: 10.1007/s11248-016-9989-6.
12. Mordhorst BR, Murphy SL, Ross RM, Samuel MS, Salazar SR, Ji TM, Behura SK, Wells KD, Green JA, Prather RS. Pharmacologic reprogramming designed to induce a warburg effect in porcine fetal fibroblasts alters gene expression and quantities of metabolites from conditioned media without increased cell proliferation. *Cell Reprogram*. 2018;20:38–48. DOI: 10.1089/cell.2017.0040.
13. Liu X, Yagi H, Saeed S, Bais AS, Gabriel GC, Chen Z, Peterson KA, Li Y, Schwartz MC, Reynolds WT, et al. The complex genetics of hypoplastic left heart syndrome. *Nat Genet*. 2017;49:1152–1159. DOI: 10.1038/ng.3870.
14. Crick SJ, Sheppard MN, Ho SY, Gebstein L, Anderson RH. Anatomy of the pig heart: comparisons with normal human cardiac structure. *J Anat*. 1998;193:105–119. DOI: 10.1046/j.1469-7580.1998.19310105.x.
15. Dhanantwari P, Lee E, Krishnan A, Samtani R, Yamada S, Anderson S, Lockett E, Donofrio M, Shiota K, Leatherbury L, et al. Human cardiac development in the first trimester: a high-resolution magnetic resonance imaging and episcopic fluorescence image capture atlas. *Circulation*. 2009;120:343–351. DOI: 10.1161/CIRCULATIONAHA.108.796698.
16. Krishnan A, Samtani R, Dhanantwari P, Lee E, Yamada S, Shiota K, Donofrio MT, Leatherbury L, Lo CW. A detailed comparison of mouse and human cardiac development. *Pediatr Res*. 2014;76:500–507. DOI: 10.1038/pr.2014.128.
17. Tsilimigras DI, Oikonomou EK, Moris D, Schizas D, Economopoulos KP, Mylonas KS. Stem cell therapy for congenital heart disease: a systematic review. *Circulation*. 2017;136:2373–2385. DOI: 10.1161/CIRCULATIONAHA.117.029607.
18. Oh H. Cell therapy trials in congenital heart disease. *Circ Res*. 2017;120:1353–1366. DOI: 10.1161/CIRCRESAHA.117.309697.
19. Gilboa SM, Devine OJ, Kucik JE, Oster ME, Riehle-Colarusso T, Nembhard WN, Xu P, Correa A, Jenkins K, Marelli AJ. Congenital heart defects in the United States: estimating the magnitude of the affected population in 2010. *Circulation*. 2016;134:101–109. DOI: 10.1161/CIRCULATIONAHA.115.019307.
20. Dennis M, Zannino D, du Plessis K, Bullock A, Disney PJS, Radford DJ, Hornung T, Grigg L, Cordina R, d'Udekem Y, et al. Clinical outcomes in adolescents and adults after the fontan procedure. *J Am Coll Cardiol*. 2018;71:1009–1017. DOI: 10.1016/j.jacc.2017.12.054.

SUPPLEMENTAL MATERIAL

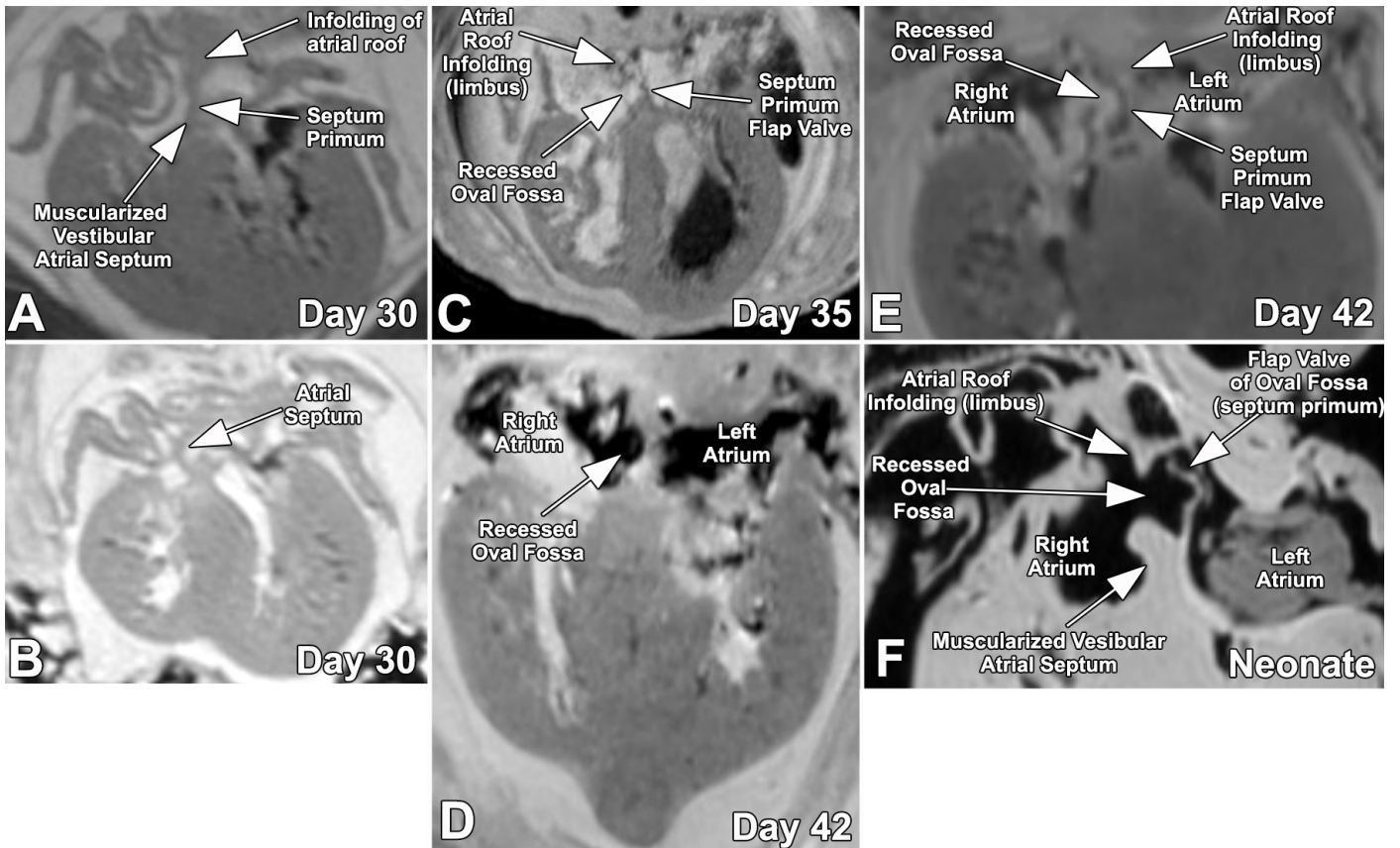


Figure S1. Developmental profile of atrial septation in the pig embryo.

A, B. Day 30 pig embryo shows no evidence of a recessed oval fossa, but the infolding of the roof of the atrial segment and the muscularized vestibular atrial part of the septum are present. The flap valve of the oval fossa is not seen at this stage.

C. Day 35 pig embryo shows a recessed oval fossa with the flap valve of the oval fossa suggesting atrial septation completion in this sample.

D, E. Day 42-pig embryo shows a recessed oval fossa, flap valve of the oval fossa and the infolding of the atrial roof forming the limbus of the oval fossa.

F. Atrial segment of the neonatal pig shows the normal atrial septum with a competent flap valve of the oval fossa.

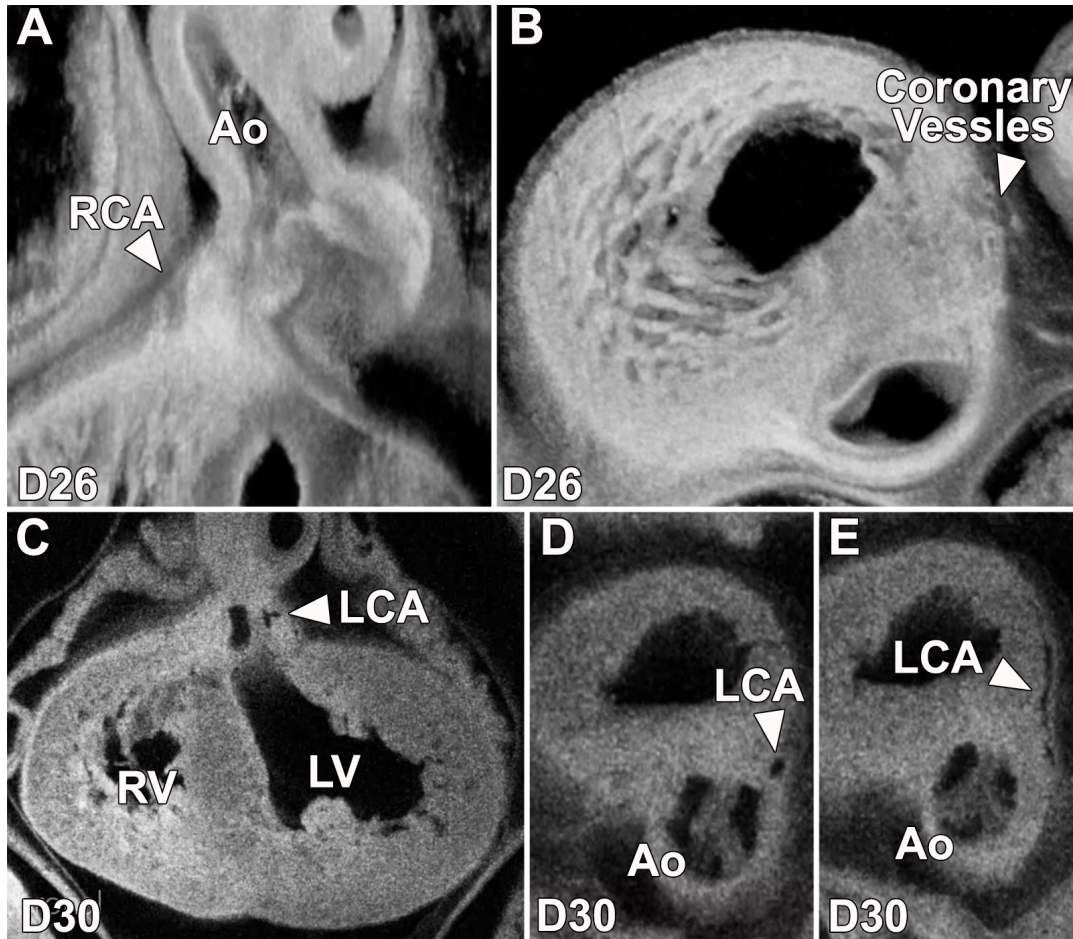


Figure S2. Development of the coronary vessels in the pig embryo. A,B. Day 26 embryo showing coronary vessels near the root of the aorta (A) and also along the epicardial surface (B)

C-E. Day 30 heart showed origin of the left coronary artery emerging inserting into the root of the aorta (C). The same specimen shown in (C) is visualized in the transverse orientation, revealing the proximal to distal progression of the left coronary artery coursing along the epicardial surface (D,E).

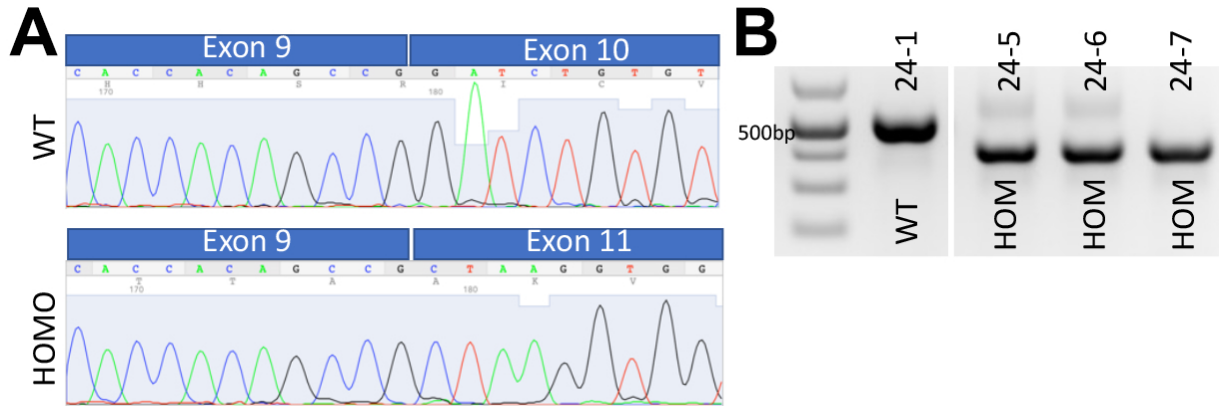


Figure S3. Pigs with CRISPR gene edited *SAP130* alleles

A. Sanger sequencing of cDNA from transcripts obtained from cells of a homozygous (HOMO) *SAP130* CRISPR gene edited pig. The edited pig expressed transcripts exhibiting the same Exon 10 skipping as previously observed in the *Ohia* HLHS mouse model¹³.

B. PCR of cDNA from transcripts from a wild type (WT) pig yielded the expected ~500 bp band, while in the three homozygous edited pig samples, only a single band is observed at ~400bp, the size expected from transcripts with the loss of exon10.

Supplemental Video Legends:

Video S1. 2D reconstruction from ECM image stack of the Day 20 pig embryo in the coronal plane. Best viewed with Windows Media Player.

Video S2. 2D reconstruction from ECM image stack of the Day 20 pig Embryo in the Transverse. Best viewed with Windows Media Player.

Video S3. 2D reconstruction from ECM image stack of the Day 20 pig embryo in the sagittal plane. Best viewed with Windows Media Player.

Video S4. 2D reconstruction from ECM image stack of the Day 26 pig embryo in the coronal plane. Best viewed with Windows Media Player.

Video S5. 2D reconstruction from ECM image stack of the Day 26 pig embryo in the transverse plane. Best viewed with Windows Media Player.

Video S6. 2D reconstruction from ECM image stack of the Day 26 pig embryo in the sagittal plane. Best viewed with Windows Media Player.

Video S7. 2D reconstruction from ECM image stack of the Day 30 pig embryo in the coronal plane. Best viewed with Windows Media Player.

Video S8. 2D reconstruction from ECM image stack of the Day 30 pig embryo in the transverse plane. Best viewed with Windows Media Player.

Video S9. 2D reconstruction from ECM image stack of the Day 30 pig embryo in the sagittal plane. Best viewed with Windows Media Player.

Video S10. 2D reconstruction from MRI image stack of the Day 42 pig embryo in the coronal plane. Best viewed with Windows Media Player.

Video S11. 2D reconstruction from MRI image stack of the Day 42 pig Embryo in the Transverse Plane. Best viewed with Windows Media Player.

Video S12. 2D reconstruction from MRI image stack of the Day 42 pig Embryo in the Sagittal Plane. Best viewed with Windows Media Player.

Video S13. 2D reconstruction from MRI image stack of the newborn pig Heart in the Coronal Plane. Best viewed with Windows Media Player.

Video S14. 2D reconstruction from MRI image stack of the newborn pig heart in the transverse plane. Best viewed with Windows Media Player.

Video S15. 2D reconstruction from MRI image stack of the newborn pig heart in the sagittal plane. Best viewed with Windows Media Player.